



OPEN ACCESS

EDITED BY

Verónica S. Di Stilio,
University of Washington, United States

REVIEWED BY

Ana Campilho,
University of Porto, Portugal
Jesse L. Labbé,
Technology Holding, United States

*CORRESPONDENCE

Shelley R. Hepworth
✉ shelley.hepworth@carleton.ca

†PRESENT ADDRESS

Gamalat Allam,
Department of Biology, Western University,
London, ON, Canada

†These authors have contributed equally to this work

RECEIVED 22 June 2023

ACCEPTED 17 October 2023

PUBLISHED 14 November 2023

CITATION

Li S, Devi B, Allam G, Bhullar A, Murmu J, Li E and Hepworth SR (2023) Regulation of secondary growth by poplar *BLADE-ON-PETIOLE* genes in Arabidopsis. *Front. Plant Sci.* 14:1244583. doi: 10.3389/fpls.2023.1244583

COPYRIGHT

© 2023 Li, Devi, Allam, Bhullar, Murmu, Li and Hepworth. This is an open-access article distributed under the terms of the [Creative Commons Attribution License \(CC BY\)](https://creativecommons.org/licenses/by/4.0/). The use, distribution or reproduction in other forums is permitted, provided the original author(s) and the copyright owner(s) are credited and that the original publication in this journal is cited, in accordance with accepted academic practice. No use, distribution or reproduction is permitted which does not comply with these terms.

Regulation of secondary growth by poplar *BLADE-ON-PETIOLE* genes in Arabidopsis

Sibei Li[†], Bhaswati Devi[†], Gamalat Allam[†], Armaan Bhullar, Jhadeswar Murmu, Eryang Li and Shelley R. Hepworth*

Department of Biology, Carleton University, Ottawa, ON, Canada

BLADE-ON-PETIOLE (*BOP*) genes are essential regulators of vegetative and reproductive development in land plants. First characterized in *Arabidopsis thaliana* (*Arabidopsis*), members of this clade function as transcriptional co-activators by recruiting TGACG-motif binding (TGA) basic leucine zipper (bZIP) transcription factors. Highly expressed at organ boundaries, these genes are also expressed in vascular tissue and contribute to lignin biosynthesis during secondary growth. How these genes function in trees, which undergo extensive secondary growth to produce wood, remains unclear. Here, we investigate the functional conservation of *BOP* orthologs in *Populus trichocarpa* (poplar), a widely-used model for tree development. Within the poplar genome, we identified two *BOP*-like genes, *PtrBPL1* and *PtrBPL2*, with abundant transcripts in stems. To assess their functions, we used heterologous assays in Arabidopsis plants. The promoters of *PtrBPL1* and *PtrBPL2*, fused with a β -glucuronidase (GUS) reporter gene showed activity at organ boundaries and in secondary xylem and phloem. When introduced into Arabidopsis plants, *PtrBPL1* and *PtrBPL2* complemented leaf and flower patterning defects in *bop1 bop2* mutants. Notably, Arabidopsis plants overexpressing *PtrBPL1* and *PtrBPL2* showed defects in stem elongation and the lignification of secondary tissues in the hypocotyl and stem. Finally, *PtrBPL1* and *PtrBPL2* formed complexes with TGA bZIP proteins in yeast. Collectively, our findings suggest that *PtrBPL1* and *PtrBPL2* are orthologs of Arabidopsis BOP1 and BOP2, potentially contributing to secondary growth regulation in poplar trees. This work provides a foundation for functional studies in trees.

KEYWORDS

BLADE-ON-PETIOLE, TGA bZIP, *Populus trichocarpa*, secondary growth, lignin

Introduction

Populus trichocarpa is a deciduous tree species that is commonly known as black cottonwood or western balsam poplar. A long-lived, mostly diploid species that is native to western North America, it is widely distributed in temperate and cold temperate regions (Cooke and Rood, 2007). *P. trichocarpa* and companion species in the genus *Populus*

(poplar) are valuable model organisms for tree research (Taylor, 2002; Jansson and Douglas, 2007). The genus is closely related to the model plant *Arabidopsis thaliana* (Arabidopsis) and many poplar gene functions are conserved. An available variety of molecular tools, such as genetic transformation methods, CRISPR-based gene editing systems, and a growing number of sequenced genomes, make poplar species ideal for molecular studies (Jansson and Douglas, 2007; Bryant et al., 2020).

BLADE-ON-PETIOLE (BOP) co-transcriptional regulators, first described in Arabidopsis, belong to a family in land plants that have a BTB/POZ (Broad-complex, Tramtrack, and Bric-a-brac/POX virus and zinc finger) domain and ankyrin repeats for interaction with other proteins (Khan et al., 2014; Backer et al., 2019). Family members are classified into two phylogenetic subclades (Khan et al., 2014; Backer et al., 2019). The first subclade contains NPR1-type proteins involved in plant defense whereas BOP-type proteins primarily regulate plant development (Khan et al., 2014; Backer et al., 2019). Proteins from both subclades lack a DNA binding domain and interact TGACG-motif binding (TGA) basic leucine zipper (bZIP) transcription factors for the co-activation or co-repression of target genes. BTB-ankyrin proteins from both subclades can also function as E3 ubiquitin ligase adaptors involved in regulating protein abundance (Fu et al., 2012; Zhang et al., 2017; Chahtane et al., 2018; He et al., 2020). In monocots and dicots, BOPs contribute to a surprisingly large number of developmental processes, including lignin deposition as a defense (Zhang et al., 2019) and during secondary growth (Khan et al., 2012b; Woerlen et al., 2017; Shen et al., 2021; Liu et al., 2022).

In Arabidopsis, *BOP1* and *BOP2* genes are strongly expressed at organ boundaries, zones that connect organs to the plant body (Žádníková and Simon, 2014; Hepworth and Pautot, 2015). These areas regulate growth at the base of organs and produce axillary meristems for the development of lateral branches, flowers, and appendages such as stipules or nectaries. Boundaries are also sites where organs separate by abscission or dehiscence to release foliage, fruits, or seeds (Hepworth and Pautot, 2015). Phenotypic defects in *bop1 bop2* double mutants are concentrated at lateral organ boundaries resulting in elongated leafy petioles, five-petaled flowers with a subtending bract, and defects in abscission (Hepworth et al., 2005; Norberg et al., 2005; McKim et al., 2008). In monocots and dicots, *BOP1* and *BOP2* paralogs participate in many of the same developmental processes (Wu et al., 2012; Tavakol et al., 2015; Couzigou et al., 2016; Jost et al., 2016; Xu et al., 2016; Toriba et al., 2019; Magne et al., 2020; Liu et al., 2022).

In Arabidopsis, *BOP1* and *BOP2* genes are also expressed in vascular tissues (Hepworth et al., 2005; Khan et al., 2012a). The overexpression of either gene inhibits stem elongation and disrupts secondary growth in stems and the root-hypocotyl (Khan et al., 2012a; Woerlen et al., 2017). In the inflorescence stem, lignified phloem and interfascicular fibers are completed earlier and the central pith becomes lignified in severe lines (Khan et al., 2012a). Secondary growth in the root-hypocotyl is also disrupted, with loss of xylem fiber differentiation (Liebsch et al., 2014; Woerlen et al., 2017). Unlike trees, secondary growth in the majority of the Arabidopsis stem is limited to the secondary thickening of xylem

and phloem cell walls and the lignification of interfascicular fibers spaced between the primary vascular bundles. These fibers complete the vascular ring and provide mechanical support (Rogers and Campbell, 2004; Ehling et al., 2005).

In woody dicot plants, cambium activity initiates in the primary vascular bundles (fascicular cambium) and spreads out to the interfascicular regions where differentiated cells regain the ability to divide (interfascicular cambium). In Arabidopsis, continuous vascular cambium only forms in the root-hypocotyl and at the base of the primary inflorescence 1–2 mm above the rosette (Sehr et al., 2010; Sanchez et al., 2012). The end result is a tube-like sheath of meristematic activity. Daughter cells on the outer rim of the cambium produce secondary phloem (inner bark) whereas daughter cells on the inside make secondary xylem (wood). In forest trees, this activity results in the radial thickening of stems and supports the development of large body architectures (Groover et al., 2006; Sehr et al., 2010; Sanchez et al., 2012).

P. trichocarpa and its relatives have emerged as an excellent platform for the study of trees (Jansson and Douglas, 2007; Bryant et al., 2020). The industrial impact of poplar is significant as hybrid poplars are among the fastest growing temperate forest trees in the world, ready for harvesting at 10 to 20 years. Trees can be grown on forest lands or marginal crop lands. Plantations, totalling some 9.6 million hectares worldwide, contribute to the storage of atmospheric CO₂ as biomass, which is harvested for the production of wood chips, plywood, biofuels, and other materials. Lignin and wood engineering in forest trees can benefit from a detailed understanding of the molecular mechanisms controlling tree architecture and wood development (Sannigrahi et al., 2010; Chanoca et al., 2019).

Here, we investigate the function of two *BOP*-like genes in *P. trichocarpa*. Highly expressed in poplar xylem and phloem, we provide evidence that these genes when heterologously expressed in Arabidopsis can function at organ boundaries and regulate lignin deposition in tissues undergoing secondary growth. We also provide evidence of complex formation with TGA bZIP proteins indicating that gene functional networks might be conserved in poplar trees. The potential evolutionary implications of these findings are discussed.

Materials and methods

Plant material and growth conditions

The *P. trichocarpa* female clone “Nisqually-1” was used (Song et al., 2006). Cuttings from a tree grown on the University of British Columbia campus (a gift of Sean Mansfield) were rooted in soil and grown under natural lighting in a greenhouse. The *Arabidopsis thaliana* Columbia (Col-0) accession was used as the wild type. The double mutant *bop1 bop2* (Hepworth et al., 2005), activation-tagged overexpression line *bop1-6D* and transgenic line *35S:BOP2* (Norberg et al., 2005) were previously described. Surface-sterilized seeds were sown on minimal media agar plates (Haughn and Somerville, 1986). Ten-day-old seedlings were planted in sterilized soil (Promix BX, Premier Tech, Quebec) supplemented

with 20-20-20 fertilizer (Plant Product Co. Ltd, Brampton, Ontario). The plants were grown to maturity in chambers at 21°C under long days (8 h dark/16 h light, intensity 100 $\mu\text{mol m}^{-2} \text{s}^{-1}$).

PtrBPL1 and *PtrBPL2* complementation of *Arabidopsis bop1 bop2* mutant

PtrBPL1 and *PtrBPL2* genes were expressed under the control of a *BOP1* promoter in *Arabidopsis bop1 bop2* mutant plants. This promoter has been previously used for complementation studies (Khan et al., 2015). The cDNA sequences of *PtrBPL1* (Potri.016G040500) and *PtrBPL2* (Potri.006G043400) were amplified by polymerase chain reaction (PCR) using cDNA from mixed poplar tissue as the template and high-fidelity iProof polymerase (Biorad, Hercules, CA). The primers annealed to the 5' and 3' untranslated regions of each gene to ensure that amplification was specific. The resulting products were cloned into pCRTM-BluntII-TOPOTM (Invitrogen, ThermoFisher Scientific, Waltham, MA) and verified by DNA sequencing (Eurofins Genomics, Louisville, KY). Verified clones were used as template to amplify the coding regions of *PtrBPL1* and *PtrBPL2* using *PtrBPL-XbaI-F* and *PtrBPL-SacI-R* as the primers. The resulting products were cloned into the corresponding sites of binary vector pBAR (a gift from the Dangl lab, University of North Carolina) downstream of the *AtBOP1* promoter (McKim et al., 2008). The resulting constructs named *BOP1p:PtrBPL1* and *BOP1p:PtrBPL2* were introduced into *Agrobacterium tumefaciens* strain C58C1 pGV101 pMP90 (Koncz and Schell, 1986). *Arabidopsis bop1 bop2* plants were transformed by floral dipping (Clough and Bent, 1998). Glufosinate-resistant primary transformant (T1) plants were selected on soil using the herbicide Finale (Bayer Environmental Sciences, Sacramento, CA). Complementation of *bop1 bop2* leaf, flower, and abscission defects was scored in the T1 generation. The progeny of ten independent T1 lines showing strong complementation were genotyped to confirm that they were *bop1 bop2* double mutants. Three to five independent transgenic lines were selected for further analysis. Primers used for cloning are listed in Supplementary Table S1.

PtrBPL1 and *PtrBPL2* promoter GUS reporter constructs

To determine the expression pattern of *PtrBPL1* and *PtrBPL2* genes, the promoters were PCR-amplified from genomic DNA template extracted from young poplar leaves using a Genomic DNA Mini Kit (Plant) (FroggaBio Inc., Concord, Ontario). A 3938-bp *PtrBPL1* promoter (nucleotides -3867 to +112) was assembled using an overlap PCR approach because the full-length sequence was difficult to amplify. A 2.9-kb *PtrBPL1* promoter fragment (nucleotides -3867 to -2876) was PCR-amplified using *ptBPL1-pro-F10* and *ptBPL1-pro-R1* as the primers. A 1.1-kb *PtrBPL1* promoter fragment (-2807 to +112) was PCR amplified using *BPL1-pro-F8* and *BPL1-May14-R* as the primers. These two

PtrBPL1 overlapping promoter fragments were gel purified, mixed, and used as template to amplify a full-length product using *PtBPL1-pro-F10* and *BPL1-May14-R* as the primer pair. The resulting *PtrBPL1* promoter (including 112-bp of *PtrBPL1* coding sequence) was column-purified and cloned into a Zero BluntTM TOPOTM vector (Invitrogen, ThermoFisher Scientific). DNA sequencing identified a 42-bp sequence deletion (nucleotides -3757 to -3715) compared to publicly available database sequence. To create the reporter gene, the *PtrBPL1* promoter was amplified from the above plasmid using *BPL1-pro-BamHI-F* and *BPL1-pro-NcoI-R* as the primer pair. The resulting product was column-purified, digested with *BamHI* and *NcoI* restriction enzymes and ligated into the corresponding sites of the pGreen-based pTGA9_{pro}:GUS plasmid (Hellens et al., 2000; Murmu et al., 2010). This ligation placed the *PtrBPL1* promoter upstream of a GUS reporter gene as a translational fusion. Similarly, a 4092-bp *PtrBPL2* promoter sequence (nucleotide -4059 to +33) was PCR-amplified using *BPL2-4kb-F* and *BPL2-Promo-R* as the primers and cloned into the Zero BluntTM TOPOTM vector (Invitrogen, ThermoFisher Scientific). The *PtrBPL2* promoter insert was then amplified using *BPL2-pro-BamHI-F* and *BPL2-pro-NcoI-R* as the primers, digested with *BamHI* and *NcoI* restriction enzymes, and cloned into the corresponding sites of pTGA9_{pro}:GUS (Murmu et al., 2010). DNA fragments destined for cloning were amplified using iProof high-fidelity polymerase (Biorad, Hercules, CA). All clones were verified by DNA sequencing (Eurofins Genomics). The resulting GUS reporter constructs were co-transformed with pSOUP into *Agrobacterium tumefaciens* strain C58C1 pGV101 pMP90 (Koncz and Schell, 1986; Hellens et al., 2000). Wild-type plants were transformed by floral dipping (Clough and Bent, 1998). Glufosinate-resistant primary transformant (T1) plants were selected on soil using the herbicide Finale (Bayer Environmental Sciences). Multiple independent transgenic lines per construct were evaluated for reporter GUS activity. Three independent transgenic lines were selected for further analysis. Primers used for cloning are listed in Supplementary Table S1.

Constructs for overexpression of *PtrBPL1* and *PtrBPL2*

The coding sequences of *PtrBPL1* and *PtrBPL2* were PCR-amplified from cloned cDNA template using iProof as the polymerase (Biorad) and *Pt6s04010CDS-F* and *Pt6s04010CDS-R* primer set, and *Pt6s04190CDS-F* and *Pt6s04190CDS-R* primer set, respectively. The resulting products were placed into the Gateway entry vector pCRTM8/GW/TOPOTM (Invitrogen, ThermoFisher Scientific) and moved into the pSM3 binary vector (Unda et al., 2017) downstream of a double 35S CaMV promoter (D35S) using GatewayTM LR ClonaseTM (Invitrogen, ThermoFisher Scientific). Wild-type plants were transformed as described above. Hygromycin-resistant primary transformants were selected on agar plates. Phenotypes were scored in the T1 generation. Three to five independent transformants were selected for further analysis. Primers used for cloning are listed in Supplementary Table S1.

Reverse transcription-quantitative PCR

Total RNA was isolated from dissected poplar tissues (a gift of the Carl Douglas lab). 2 µg of RNA was used for cDNA synthesis using Superscript III reverse transcriptase (Invitrogen, ThermoFisher Scientific). PCR reactions in triplicate containing 2 µl of 10-fold diluted cDNA, gene-specific primers (Supplementary Table S1) and Power SYBRTM Green Master mix (Invitrogen, ThermoFisher Scientific) were carried out using a StepOnePlus thermocycler (Applied Biosystems, ThermoFisher Scientific). Relative transcript levels were calculated according to Pfaffl (2001). Values were normalized to the poplar elongation factor reference gene *C672* (Wang et al., 2014) and then to young leaf. Data are the average of four measurements for each of two biological replicates. Error bars show standard deviation.

Localization of lignin deposition

Tissues were analyzed for lignin deposition as previously described (Khan et al., 2012b; Woerlen et al., 2017). Arabidopsis stems were harvested from five-week-old plants. A razor blade was used to hand-cut sections from the base of the primary inflorescence about 1 cm above the rosette leaves (Khan et al., 2012b). Hypocotyls were harvested from seven-week-old plants. A razor blade was used to hand-cut sections about 1.5 mm below the rosette leaves. Samples were placed in 2% phloroglucinol dissolved in 95% ethanol for five minutes. Then, five drops of concentrated hydrochloric acid were added. Two minutes were allowed for color development. Immediately, samples were transferred onto a glass slide and a cover slip was added. Images were collected using a Discovery V20 stereomicroscope (Carl Zeiss Canada, North York, Ontario).

Localization of GUS activity

Tissues were analyzed for β-glucuronidase (GUS) activity as previously described (Woerlen et al., 2017) with minor changes. The staining solution contained 4 mM KFe(CN) and 2 mM of 5-bromo-4-chloro-3-indoxyl-β-D-glucuronide (X-Gluc). The samples were incubated at 37°C for 3 to 24 hours until a localized blue precipitate was visible. After clearing in 70% ethanol, the samples were imaged using a Discovery V20 stereomicroscope (Carl Zeiss). For sections, the stained tissue was embedded in Paraplast Plus[®] (Sigma-Aldrich, St. Louis, MO) and processed using *tert*-butanol instead of xylenes (Woerlen et al., 2017). Tissue sections (20 µm) were fixed onto glass slides and dewaxed with *tert*-butanol. The samples were imaged using an Axio Imager M2 compound microscope (Carl Zeiss).

Yeast two-hybrid assay

Protein-protein interactions were assayed using a MatchmakerTM GAL4-based yeast two-hybrid system (Clontech, Takara Bio USA Inc,

San Jose, CA) and Gateway-compatible pGBKT7-DEST (bait) and pGADT7-DEST (prey) plasmids modified from pGBKT7 and pGADT7-Res vectors, respectively (Lu et al., 2009). PtrBPL1 and PtrBPL2 proteins fused to the DNA-binding domain of yeast GAL4 were used as bait. AtTGA1, AtTGA4, AtTGA3, AtTGA7 and AtTGA8/PAN proteins fused to the transcriptional activation domain of yeast GAL4 were used as prey. To prepare Gateway entry vectors, the full-length coding sequences of bait and prey genes were cloned into pCRTM8/GW/TOPOTMTA (Invitrogen, ThermoFisher Scientific). All entry vector inserts were sequenced to confirm authenticity. To make the final plasmids, recombination reactions were performed using GatewayTM LR ClonaseTM II enzyme mix according to the manufacturer's instructions (Invitrogen, ThermoFisher Scientific). Bait and prey plasmid were co-transformed into yeast AH109 strain (Gietz and Schiestl, 2007). Transformed yeast colonies were identified by selection on synthetic complete (SC) media plates lacking Leu and Trp (SC/-Leu/-Trp). Dilution series were spotted onto SC/-Leu/-Trp medium or SC/-Leu-Trp-His medium plus 10 mM 3-amino-1,2,4-triazole (3-AT; Sigma-Aldrich) for assessment of His reporter gene activity. A 3-AT concentration (10 mM) sufficient to distinguish positive growth from background was determined empirically.

Bioinformatics

P. trichocarpa homologs of Arabidopsis BTB-ankyrin and TGA bZIP proteins were identified using the plant homologs tool at The Arabidopsis Information Resource (TAIR) (www.arabidopsis.org). The corresponding *P. trichocarpa* protein sequences were retrieved from Phytozome (Goodstein et al., 2012; phytozome-next.jgi.doe.gov). MEGA version 11 was used for the alignment of protein sequences by MUSCLE (Edgar, 2004) using the default parameters (www.megasoftware.net). Maximum Likelihood trees were constructed based on 100 bootstrap replicates using the Jones-Taylor-Thornton Model. The BOXSHADE alignment and sequence logos were prepared using Geneious Prime 2022.1 (www.geneious.com). The percent similarity of protein pairs was calculated using the Expasy SIM tool (www.expasy.org/sim).

Promoter analysis

The 500-bp promoter sequences upstream of the translational start sites of *AtBOP1*, *AtBOP2*, *PtrBPL1*, and *PtrBPL2* genes were retrieved from their genome assemblies found at TAIR (<https://www.arabidopsis.org/>) or Phytozome (<https://phytozome-next.jgi.doe.gov/>). Scanning for Transcription Factor Binding Sites (TFBS) was carried out using PlantPAN 3.0 (<http://plantpan.itps.ncku.edu.tw/index.html>). Selected TFBS were aligned to statistically enriched 6-mers identified by the motif finder tool at TAIR. Binding site locations were visualized by using TBtools v1.123 (Chen et al., 2020).

Results

Identification of BTB-ankyrin and TGA bZIP gene families in poplar

In the *P. trichocarpa* (poplar) genome, six BTB-ankyrin proteins were identified. The phylogenetic relationship Arabidopsis and poplar BTB-ankyrin proteins was investigated (Figure 1A). This analysis revealed one NPR1 protein (Potri.006G148100), three NPR3/4 proteins (Potri.012G118300; Potri.012G118500; Potri.015G117200) and two poplar BOP-like proteins designated as PtrBPL1 (Potri.016G040500) and PtrBPL2 (Potri.006G043400), respectively. Multiple sequence alignment showed that PtrBPL1 and PtrBPL2 are 94.3% similar to each other at the amino acid level and 80.2% versus 75.6% similar to AtBOP1, respectively. The similarity is broadly distributed across the length of the proteins, not just within the BTB/POZ and ankyrin repeat domain (Figures 1B–D; Supplementary Figure S1). Less conserved regions are situated within the BTB/POZ domain and near the C-terminus. For example, PtrBPL1 contains a deletion in the C-terminus compared to AtBOP1/2 and PtrBPL2 proteins (Figure 1B; Supplementary Figure S1). In parallel, we investigated the phylogenetic relationship of poplar TGA bZIP proteins as potential functional partners. Representatives from all five TGA clades found in Arabidopsis are present (Figure 1E; Supplementary Figure S2). Given these overall

similarities, we anticipated that PtrBPL1 and PtrBPL2 might have conserved activities similar to AtBOP1 and AtBOP2.

PtrBPL1 and PtrBPL2 expression pattern

We next obtained expression data for *PtrBPL1* and *PtrBPL2* from the Bio-Analytic Resource for Plant Biology (BAR, www.utoronto.ca/bar). These data showed the wide expression of both genes in poplar tissues including seedlings, young leaves, catkins, roots, and xylem (Figures 2A, B). We then used RT-qPCR to monitor transcript abundance in selected tissues. These data showed that *PtrBPL1* and *PtrBPL2* transcripts are enriched in the petiole region of leaves compared to the blade. Significant expression was also observed in xylem and phloem tissues of young poplar stems (Figure 2C).

We next investigated the spatial and temporal expression of *PtrBPL1* and *PtrBPL2* genes, by monitoring the expression of *PtrBPL1p:GUS* and *PtrBPL2p:GUS* reporter genes in Arabidopsis plants (Figure 2D). In seedlings, both genes were expressed in boundaries at the base of the cotyledons. During flowering, both genes were expressed at nodes in the stem where a boundary forms at the base of the flower pedicel. GUS expression was evident in floral organ boundaries and abscission zones at the base of young silicles for *PtrBPL1* but not *PtrBPL2* (Supplementary Figure S3). The vasculature of cotyledons, leaves, and the hypocotyl also showed differential expression. *PtrBPL2* but not *PtrBPL1* was expressed

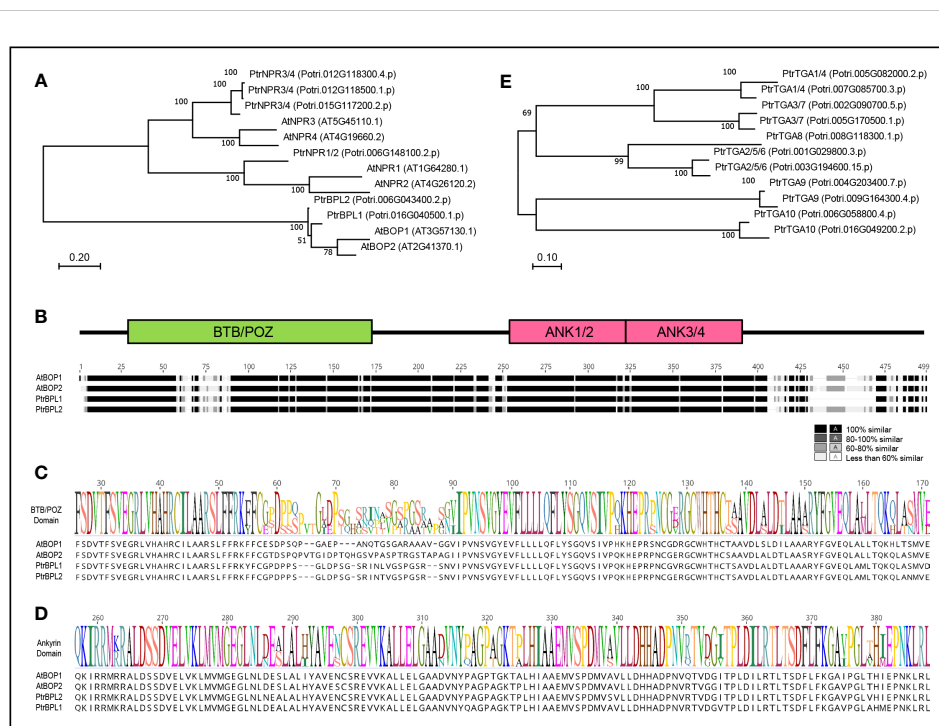


FIGURE 1

Proteins encoded by BTB-ankyrin and TGA bZIP genes from Arabidopsis and poplar. (A) Maximum Likelihood tree showing phylogenetic relationships between Arabidopsis (At) and poplar (Ptr) BTB-ankyrin proteins. (B) Multiple sequence alignment of ATBOP and PtrBPL proteins with corresponding domain map showing the relative position of conserved BTB/POZ and ankyrin (ANK) domains. Segments of highest similarity or identity are colored darkest and segments of lowest identity or similarity are colored lightest. (C) BTB/POZ domain sequence logo. (D) Ankyrin domain sequence logo. Protein sequences with listed identification numbers were retrieved from TAIR (www.arabidopsis.org) or Phytosome (phytosome-next.jgi.doe.gov). (E) Maximum Likelihood tree showing phylogenetic relationships between PtrTGA proteins.

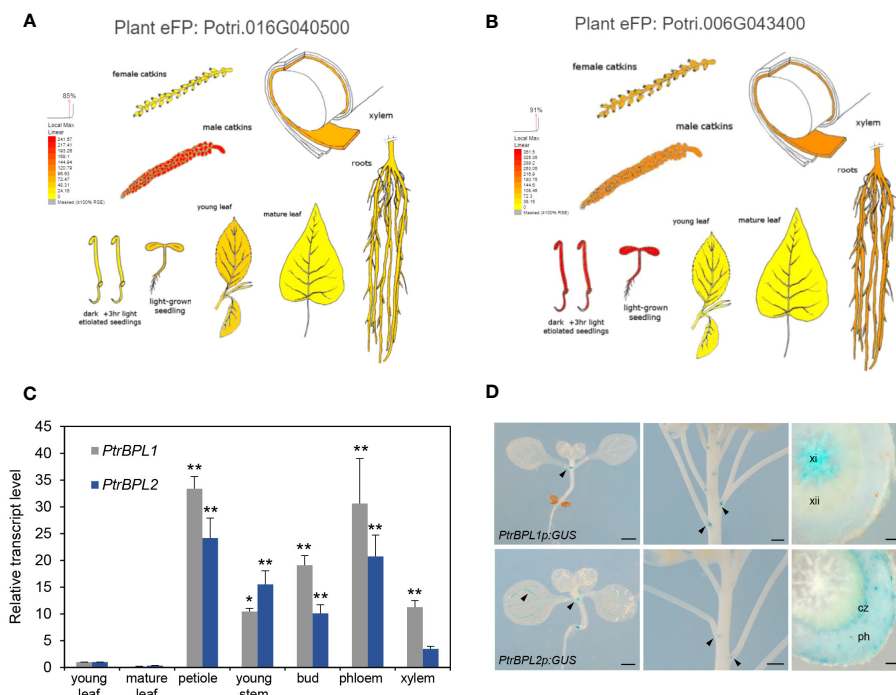


FIGURE 2

Expression of *PtrBPL1* and *PtrBPL2* in poplar and Arabidopsis. (A, B) Transcriptome data for *P. trichocarpa* compiled by the Bio-Analytic Resource for Plant Biology (www.bar.utoronto.ca). Red, high expression; orange, medium expression; yellow, lower expression. Plant eFP viewer output for (A) *PtrBPL1* and (B) *PtrBPL2*. (C) The relative abundance of *PtrBPL1* and *PtrBPL2* transcript was independently measured using RT-qPCR in dissected poplar tissues. Data are the average \pm SD of four measurements performed on each of two biological replicates. Values were normalized to young leaf. Asterisks indicate significant differences between tissues compared with young leaf (ANOVA with Tukey's test, ** $P < 0.01$, * $P < 0.05$). (D) Expression patterns of *PtrBPL1p:GUS* and *PtrBPL2p:GUS* in Arabidopsis seedlings, inflorescences, and sectioned hypocotyls. Arrows denote expression at organ boundaries. xi, secondary xylem I; xii, secondary xylem II; ph, secondary phloem; cz, cambium zone. Scale bars, 500 μ m except 100 μ m for hypocotyl sections.

in veins of leaves (Figure 2D; Supplementary Figure S3). At the seedling stage, both genes were expressed at the root tip and at the base of lateral roots (Supplementary Figure S3). In the hypocotyl, *PtrBPL1* was strongly expressed in early secondary xylem (xylem I) whereas *PtrBPL2* was expressed at the outer edge of the cambial zone and in secondary phloem (Figure 2D; Supplementary Figure S3). Neither *AtBOP1* nor *AtBOP2* are expressed in secondary xylem (Liebsch et al., 2014; Woerlen et al., 2017) indicating a possible difference in gene regulation between the two species. To investigate this difference, a statistical motif analysis was carried out using the promoter regions (500 base pairs upstream of the start codon) of all four genes. This analysis showed an enrichment of MYB-related and NAC transcription factor binding sites in the promoters of *PtrBPL1* and *PtrBPL2* compared to *AtBOP1* and *AtBOP2* (Supplementary Figure S4) implicating these factors in the differential regulation of poplar orthologs.

PtrBPL1 and *PtrBPL2* can complement *bop1 bop2* leaf and flower patterning defects

To investigate to what extent *PtrBPL1* and *PtrBPL2* can substitute for *AtBOP1* and *AtBOP2*, we expressed *PtrBPL1* and *PtrBPL2* under the control of an *AtBOP1* promoter in *bop1 bop2*

mutants and tested for complementation. In total, we obtained 203 primary (T1) transformants for *BOP1p:PtrBPL1* and 212 primary transformants for *BOP1p:PtrBPL2* (Supplementary Table S2). Characteristic defects in *bop1 bop2* mutants include leafy petioles, loss of floral organ abscission, and flowers with a bract and extra petals on the abaxial side (Hepworth et al., 2005). Strong or medium complementation of the leaf phenotype was observed in 54% and 52% of *PtrBPL1* and *PtrBPL2* transformants, respectively (Figure 3; Supplementary Table S2). Floral patterning defects were significantly restored in 65% and 76% of *PtrBPL1* and *PtrBPL2* transformants scored, respectively (Supplementary Table S2). Floral organ abscission was significantly restored in 76% and 62% of *PtrBPL1* and *PtrBPL2* transformants scored, respectively (Figure 3; Supplementary Table S2). These data confirm that heterologous expression of *PtrBPL1* and *PtrBPL2* can complement *bop1 bop2* mutant phenotypes.

Overexpression of *PtrBPL1* and *PtrBPL2* alters secondary growth

Plants that overexpress *AtBOP1* or *AtBOP2* are short and bushy, with a wider pattern of secondary lignin deposition in stems (Khan et al., 2012b). Unlike trees, a continuous vascular cambium does not

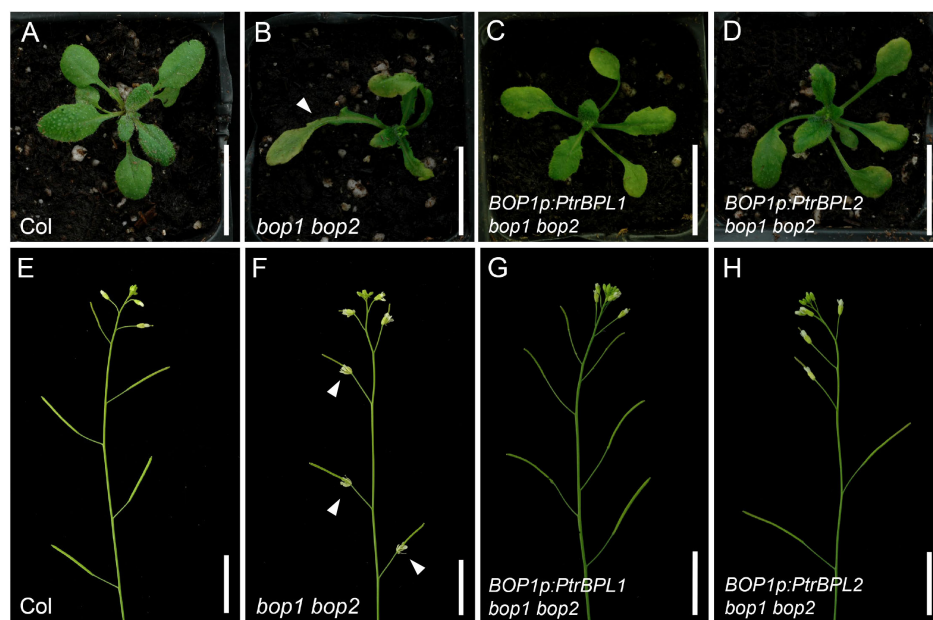


FIGURE 3

Complementation of Arabidopsis *bop1 bop2* leaf and flower defects with *PtrBPL1* and *PtrBPL2*. *PtrBPL1* and *PtrBPL2* coding regions were expressed under the control of the *AtBOP1* promoter in *bop1 bop2* plants. Representative plants are shown in the T2 generation. See [Supplementary Table S2](#) for quantitative analysis of complementation for *bop1 bop2* defects in leaf morphology, floral patterning, and abscission. (A, B) Wild-type plant showing (A) smooth leaf petioles and (B) inflorescence with floral organ abscission. (C, D) A *bop1 bop2* mutant showing (C) leaves with a blade-on-petiole phenotype (arrow) and (D) inflorescence with asymmetric flowers and loss of floral organ abscission (arrows). (E, F) A *BOP1p:PtrBPL1 bop1 bop2* plant showing (E) smooth leaf petioles and (F) inflorescence with floral organ abscission restored. (G, H) A *BOP1p:PtrBPL2 bop1 bop2* plant showing (G) smooth leaf petioles and (H) inflorescence with floral organ abscission restored. Scale bars, 1.5 cm.

form except at the base of the stem. Instead, secondary growth is evident as the differentiation of abundant lignified interfascicular fibers (Ehlting et al., 2005).

To test the effect of *PtrBPL1* and *PtrBPL2* on stem development, Arabidopsis plants were transformed with a construct driving *PtrBPL1* and *PtrBPL2* expression from a strong, constitutive double cauliflower mosaic virus 35S promoter (*D35S*). Flowering *D35S:PtrBPL1* and *D35S:PtrBPL2* plants showed a loss of apical dominance and reduced stature in comparison to wild-type plants (Figure 4; [Supplementary Table S3](#)). The stems of 5-6 representative *D35S:PtrBPL1* and *D35S:PtrBPL2* plants were hand-sectioned and stained with phloroglucinol to test for changes in lignin deposition. Several plants in this population showed an expanded pattern of lignin deposition in stems.

In the root-hypocotyl where a continuous vascular cambium forms, two phases of secondary growth take place (Chaffey et al., 2002; Nieminen et al., 2015). During the first phase, the xylem I is composed of lignified vessel cells in a matrix of non-lignified parenchyma. Flowering triggers the second phase, in which xylem II forms as a thick ring composed of lignified fibers interspersed with lignified vessels (Chaffey et al., 2002; Nieminen et al., 2015). Arabidopsis plants that overexpress *AtBOP1* and *AtBOP2* lack xylem II features in the upper part of the root (Woerlen et al., 2017) and hypocotyl (Liebsch et al., 2014).

Analysis of secondary growth in the hypocotyl of *D35S:PtrBPL1* and *D35S:PtrBPL2* lines showed at least one *D35S:PtrBPL1* line (n=3)

missing xylem II fibers and vessels similar to *bop1-6D* and *35S:BOP2* control plants (Figure 4; [Supplementary Figure S5](#)). The xylem II ring in all *D35S:PtrBPL2* lines (n=3) was reduced in thickness compared to wild-type control plants. These data provide further evidence that *PtrBPL1* and *PtrBPL2* can functionally substitute in Arabidopsis plants.

PtrBPL1 and PtrBPL2 interact with TGA bZIP factors

BTB-ankyrin proteins perform a variety of function by utilizing TGA bZIP factors as interaction partners (Backer et al., 2019). For example, Arabidopsis BOP1 and BOP2 interact with clade I and clade III TGAs in yeast (Hepworth et al., 2005). Such complexes are implicated in the regulation of stem development and lignin deposition in plants (Wang et al., 2019; Zhang et al., 2019). Arabidopsis BOP1 and BOP2 also interact with PAN/TGA8 for patterning functions in the flower (Hepworth et al., 2005). A highly sensitive method for detecting protein-protein interactions, we used the yeast two-hybrid assay to assess PtrBPL interactions with AtTGA factors. PtrBPL1 and PtrBPL2 fused to the DNA-binding domain of the yeast transcription activator protein GAL4 were used as bait. AtTGA1, AtTGA4, AtTGA3, and AtTGA7 fused to the activation domain of GAL4 were used as prey. Figure 5 shows that PtrBPL1 and PtrBPL2 interact with AtTGA1, AtTGA4, AtTGA3, and AtTGA7 providing evidence of conserved functional partners in Arabidopsis and poplar.

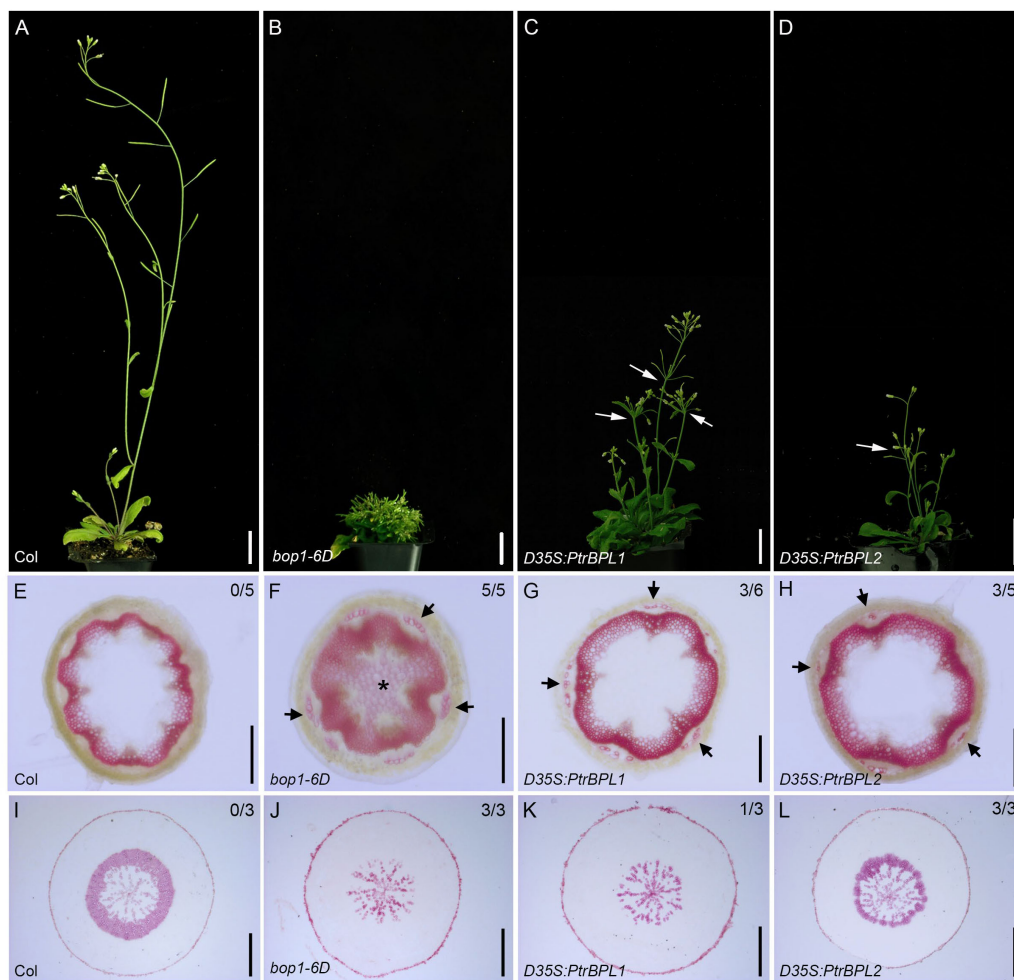


FIGURE 4

Overexpression of *PtrBPL1* and *PtrBPL2* in Arabidopsis plants. *PtrBPL1* and *PtrBPL2* coding regions were expressed under the control of a double 35S (*D35S*) cauliflower mosaic virus promoter in wild-type Arabidopsis plants. (A–D) Representative flowering plants are shown in the T1 generation. See Supplementary Table S3 for quantitative analysis. (A) Wild type plant, showing strong apical dominance and elongated internodes. (B) *bop1-6D* plant, showing a bushy, dwarf stature. (C) *D35S:PtrBPL1* plant, showing a bushy, semi-dwarf stature. Arrows, clustered flowers and siliques. (D) *D35S:PtrBPL2* plant, showing a bushy, semi-dwarf stature. Arrows, clustered flowers and siliques. (E–H) Transverse sections from the base of fully elongated stems were stained phloroglucinol-HCl to reveal lignin (pink). Top left, number of independent transgenic lines showing abnormal lignin deposition. Representative sections are shown for: (E) wild-type stem, showing a continuous vascular ring. (F) *bop1-6D* stem, showing a thicker vascular ring, lignified pith (asterisk) and lignified phloem fibers (arrows) (G) *D35S:PtrBPL1* stem, showing a thick vascular ring and lignified phloem fibers (arrows). (H) *D35S:PtrBPL2* stem, showing a thick vascular ring and lignified phloem fibers (arrows). (I–L) Transverse sections from the middle of the hypocotyl (1.5 mm below the rosette leaves) were stained phloroglucinol-HCl to reveal lignin (pink). Top left, number of independent transgenic lines showing abnormal lignin deposition. Representative sections are shown for: (I) Wild-type hypocotyl, showing a thick ring of xylem II. (J) *bop1-6D* hypocotyl, showing a lack of xylem II fibers and vessels. (K) *D35S:PtrBPL1* hypocotyl, showing a lack of xylem II fibers and vessels. (L) *D35S:PtrBPL2* hypocotyl, showing a xylem II ring of reduced thickness, compared to the wild type. Scale bars: (A–D) 1.5 cm; (E–H) 0.25 mm; (I–L) 0.5 mm.

Discussion

Trees display prominent radial growth in the stem in which secondary xylem and phloem tissues are produced by the vascular cambium. Current knowledge regarding the genetic regulation of cambium activity and secondary growth is still incomplete (Wang et al., 2021). Therefore, understanding gene families potentially involved in this process is desirable.

The BOP family of co-transcriptional regulators are conserved in dicots and monocots and contribute to numerous developmental processes. Studies in dicots such as tobacco (Wu et al., 2012),

legumes (Frankowski et al., 2015; Couzigou et al., 2016; Magne et al., 2018), tomato (Xu et al., 2016; Izhaki et al., 2018) and monocots such as rice (Toriba et al., 2020), barley (Tavakol et al., 2015; Jost et al., 2016) and *Brachypodium* (Magne et al., 2020; Liu et al., 2022) reveal highly conserved functions, comparable to Arabidopsis, that influence organ patterning, inflorescence architecture, and abscission (Khan et al., 2014; Hepworth and Pautot, 2015). Taxon-specific roles in the maintenance of symbiotic nodule identity (Couzigou et al., 2012; Magne et al., 2018) and rhizome development (Toriba et al., 2020) have also been identified.

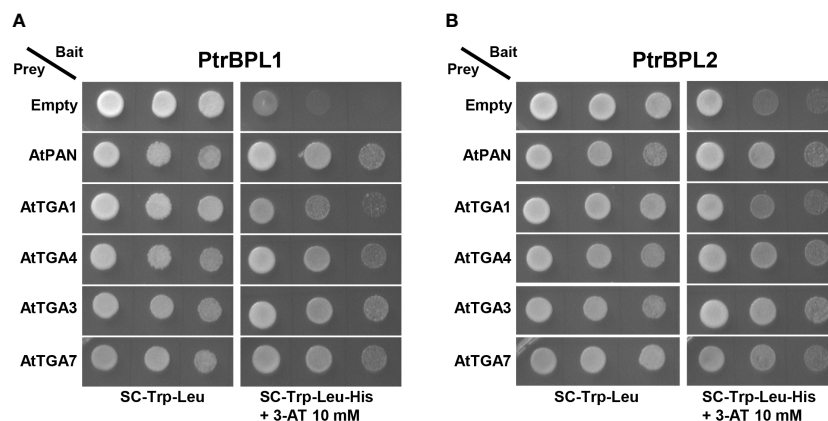


FIGURE 5

Pair-wise yeast two-hybrid assays showing (A) *PtrBPL1* and (B) *PtrBPL2* interaction with AtTGAs. *PtrBPL1* and *PtrBPL2* baits were fused to the DNA-binding domain of yeast GAL4. AtTGA1, AtTGA4, AtTGA3, and AtTGA7 preys were fused to the transcriptional activation domain of yeast GAL4. Plasmid constructs were co-transformed into yeast AH109 strain before serial dilutions (10^{-1} , 10^{-2} , 10^{-3}) were plated onto SC/-Trp/-Leu medium with or without histidine + 10 mM 3-AT. Growth on SC/-Trp/-Leu/-His/+3-AT above background confirms a protein-protein interaction. Dilutions were spotted in replicate onto SC/-Trp/-Leu/-His/+3-AT medium. Photos on SC/-Trp/-Leu were taken three days after plating. For all assays, interaction with AtPAN/TGA8 was used as a positive control and an empty prey vector was used as a negative control.

In flowering plants, BOPs are involved in boundary formation. These specific domains are important for the separation of meristematic regions from lateral organs (Aida and Tasaka, 2006; Žádníková and Simon, 2014). Compared to the shoot apical meristem, our knowledge of boundaries and their involvement in cambium meristems is limited. The conservation of BOPs across the plant kingdom (Khan et al., 2014) makes it plausible that orthologs in trees have roles in the vascular cambium and secondary growth.

The results shown here indicate that *PtrBPL1* and *PtrBPL2* play a role in secondary growth when overexpressed in Arabidopsis. *D35S:PtrBPL1* and *D35S:PtrBPL2* transgenic plants were characterized by dwarf stems with a thicker vascular ring and more developed phloem fibers whereas the increased activity of these genes in the hypocotyl interfered with xylem II production. Overexpression of either *PtrBPL1* or *PtrBPL2* resulted in phenotypes that were highly similar to those observed in Arabidopsis plants with overexpression of *AtBOP1* or *AtBOP2* (Khan et al., 2012b; Woerlen et al., 2017). Furthermore, the expression of *PtrBPL1* or *PtrBPL2* transgenes in a *bop1 bop2* mutant background was sufficient to rescue leaf and floral patterning defects. Abscission defects in the *bop1 bop2* mutant were also corrected. The *PtrBPL1p:GUS* and *PtrBPL2p:GUS* expression patterns in Arabidopsis plants were consistent with a role in boundary patterning and secondary growth. Finally, we identified a family of TGA bZIP factors in poplar with a clade structure similar that in Arabidopsis plants. Yeast two hybrid assays indicated that *PtrBPL1* and *PtrBPL2* can interact with AtTGAs known to mediate roles in plant development and lignin deposition. All of these results strongly suggest that BOP1/2-TGA modules characterized in Arabidopsis are conserved in *P. trichocarpa*. Therefore, it is feasible they contribute to stem development in trees.

In Arabidopsis plants, *BOP1* and *BOP2* genes are repressed by the class I KNOX homeodomain transcription factors SHOOT

MERISTEMLESS (STM) and BREVIPEDICELLUS (BP) during meristem maintenance, stem development, and secondary xylem formation (Jun et al., 2010; Khan et al., 2012b; Liebsch et al., 2014; Khan et al., 2015; Woerlen et al., 2017). Consistent with these findings, *PtrBPL1* is significantly downregulated in the stem of hybrid poplar overexpressing the STM ortholog ARBORKNOX1 (ARK1) (Liu et al., 2015). Both ARK1 and ARK2 (ortholog of BP) are strongly expressed in the cambial zone (Groover et al., 2006; Du et al., 2009). In the ARK1 overexpressor, the boundary between the cambium and the secondary xylem was uneven and phloem fibers were reduced in number (Groover et al., 2006). In the ARK2 overexpressor, extra secondary phloem was produced at the expense of phloem fibers and secondary xylem leading to an overall decrease in the differentiation of lignified cell-types. Conversely, an *ark2* mutant generated by artificial miRNA silencing showed a premature differentiation of secondary xylem and phloem fibers, similar to the *bp* mutant in Arabidopsis (Du et al., 2009).

Studies in the tropical Cannabaceae tree *Parasponia andersonii* species complement these findings (Shen et al., 2021). CRISPR-Cas9 loss-of-function mutants in the *AtBOP1* ortholog *PanNODULE ROOT1* (*PanNOOT1*) were altered in the development of xylem and phloem tissues without any obvious difference in cambium organization and size. Compared to the wild-type, the differentiation of secondary xylem and phloem was inhibited resulting in a reduced stem diameter. Transcriptomic data showed a reduction in the expression of lignin metabolism-related genes (Shen et al., 2021). In both Arabidopsis and cotton (*Gossypium hirsutum*) and the grass *Brachypodium distachyon* model, BOPs positively regulate the expression of lignin biosynthesis genes and lignin deposition in stems (Khan et al., 2012b; Zhang et al., 2019; Liu et al., 2022).

In Arabidopsis plants, *BOP1* and *BOP2* promote the expression of two homeobox genes to influence lignin deposition (Khan et al.,

2012a; Khan et al., 2012b; Woerlen et al., 2017). Poplar plants contain homeobox genes that are highly similar to *ARABIDOPSIS HOMEBOX GENE 1 (ATH1)* (Potri.018G054700/Potri.006G230700) and *KNOTTED-LIKE FROM ARABIDOPSIS THALIANA 6 (KNAT6)* (Potri.010G043500/Potri.008G188700) suggesting that downstream pathway components are conserved. The homologous genes in *P. andersonii* were significantly downregulated in *Pannoot1* stems showing a similar regulation as in Arabidopsis plants (Shen et al., 2021). The *PagKNAT2/6b* gene from a hybrid poplar clone (*P. alba* X *P. glandulosa*) is highly expressed in xylem and phloem. Compared to controls plants, transgenic poplar clones overexpressing *PagKNAT2/6b* showed a reduction in xylem formation by negatively regulating the expression of NAC domain transcription factor genes including *PagXYLEM NAC DOMAIN 1* as a direct target (Zhao et al., 2020).

Spatial and temporal differences between *PtrBPL1p:GUS* and *PtrBPL2p:GUS* expression were observed. In Arabidopsis plants, the *PtrBPL1* promoter was active in xylem I whereas *PtrBPL2* the promoter was active at the boundary of the cambial zone and secondary phloem (Figures 2A, B, D). By contrast, a *PanNOOT1p:GUS* reporter was expressed in all three tissues during secondary growth (Shen et al., 2021). A similar pattern to *PanNOOT1* was detected in aspen (*P. tremula*) and birch (*Betula pendula*) using high-spatial-resolution gene expression mapping (Sundell et al., 2017; Alonso-Serra et al., 2019; Shen et al., 2021). By contrast, *AtBOP1p:GUS* and *AtBOP2p:GUS* expression is normally repressed by BP in the cambial zone and secondary xylem of the root and hypocotyl (Liebsch et al., 2014; Khan et al., 2015; Woerlen et al., 2017). Thus, divergent transcriptional regulation may account for phenotypic differences in secondary growth between species. Compared to *AtBOP1* and *AtBOP2*, the *PtrBPL1* and *PtrBPL2* promoters had a higher number of predicted binding sites for MYB-related and NAC transcription factors, which as a group contribute strongly to secondary growth in plants (Nakano et al., 2015).

Considering all of the above, BOP-TGA modules characterized in Arabidopsis are likely conserved in poplar. Information gained from this study forms a basis for further exploration of networks that regulate cambium development and secondary growth in trees.

Data availability statement

The raw data supporting the conclusions of this article will be made available by the authors, without undue reservation.

References

- Aida, M., and Tasaka, M. (2006). Genetic control of shoot organ boundaries. *Curr. Opin. Plant Biol.* 9, 72–77. doi: 10.1016/j.pbi.2005.11.011
- Alonso-Serra, J., Safronov, O., Lim, K. J., Fraser-Miller, S. J., Blokhina, O. B., Campilho, A., et al. (2019). Tissue-specific study across the stem reveals the chemistry and transcriptome dynamics of birch bark. *New Phytol.* 222, 1816–1831. doi: 10.1111/nph.15725
- Backer, R., Naidoo, S., and van den Berg, N. (2019). The NONEXPRESSOR OF PATHOGENESIS-RELATED GENES 1 (NPR1) and related family: mechanistic insights in plant disease resistance. *Front. Plant Sci.* 10. doi: 10.3389/fpls.2019.00102
- Bryant, N. D., Pu, Y., Tschaplinski, T. J., Tuskan, G. A., Muchero, W., Kalluri, U. C., et al. (2020). Transgenic poplar designed for biofuels. *Trends Plant Sci.* 25, 881–896. doi: 10.1016/j.tplants.2020.03.008
- Chaffey, N., Cholewa, E., Regan, S., and Sundberg, B. (2002). Secondary xylem development in Arabidopsis: a model for wood formation. *Plant Physiol.* 114, 594–600. doi: 10.1034/j.1399-3054.2002.1140413.x
- Chahtane, H., Zhang, B., Norberg, M., Lemasson, M., Thévenon, E., Bakó, L., et al. (2018). LEAFY activity is post-transcriptionally regulated by BLADE ON PETIOLE2 and CULLIN3 in Arabidopsis. *New Phytol.* 220, 579–592. doi: 10.1111/nph.15329

Author contributions

SH and EL designed the research. SL, BD, GA, JM, and EL performed the research. AB carried out bioinformatics analysis. SL, JM, and SH wrote the article. All authors contributed to the article and approved the submitted version.

Funding

This work was supported by a Discovery Grant from the Natural Sciences and Engineering Research Council (NSERC) of Canada (RGPIN-2016-06193).

Acknowledgments

We thank Carl Douglas and Shawn Mansfield at the University of British Columbia for the gift of poplar cuttings, vectors, and poplar tissue cDNA. We thank Ying Wang and Kevin Xiong for help with cloning and Jenna O'Neill for images of GUS-stained seedlings.

Conflict of interest

The authors declare that the research was conducted in the absence of any commercial or financial relationships that could be construed as a potential conflict of interest.

Publisher's note

All claims expressed in this article are solely those of the authors and do not necessarily represent those of their affiliated organizations, or those of the publisher, the editors and the reviewers. Any product that may be evaluated in this article, or claim that may be made by its manufacturer, is not guaranteed or endorsed by the publisher.

Supplementary material

The Supplementary Material for this article can be found online at: <https://www.frontiersin.org/articles/10.3389/fpls.2023.1244583/full#supplementary-material>

- Chanoca, A., de Vries, L., and Boerjan, W. (2019). Lignin engineering in forest trees. *Front. Plant Sci.* 10. doi: 10.3389/fpls.2019.00912
- Chen, C., Chen, H., Zhang, Y., Thomas, H. R., Frank, M. H., He, Y., et al. (2020). TBtools: an integrative toolkit developed for interactive analyses of big biological data. *Mol. Plant* 13, 1194–1202. doi: 10.1016/j.molp.2020.06.009
- Clough, S. J., and Bent, A. F. (1998). Floral dip: a simplified method for *Agrobacterium*-mediated transformation of *Arabidopsis thaliana*. *Plant J.* 16, 735–743. doi: 10.1046/j.1365-313x.1998.00343.x
- Cooke, J. E. K., and Rood, S. B. (2007). Trees of the people: the growing science of poplars in Canada and worldwide. *Can. J. Bot.* 85, 1103–1110. doi: 10.1139/b07-125
- Couzigou, J. M., Magne, K., Mondy, S., Cosson, V., Clements, J., and Ratet, P. (2016). The legume *NOOT-BOP-COCH-LIKE* genes are conserved regulators of abscission, a major agronomical trait in cultivated crops. *New Phytol.* 209, 228–240. doi: 10.1111/nph.13634
- Couzigou, J. M., Zhukov, V., Mondy, S., Heba, G. A., Cosson, V., Noel Ellis, T. N., et al. (2012). *NODULE ROOT* and *COCHLEATA* maintain nodule development and are legume orthologs of Arabidopsis *BLADE-ON-PETIOLE* genes. *Plant Cell* 24, 4498–4510. doi: 10.1105/ypc.112.103747
- Du, J., Mansfield, S. D., and Groover, A. T. (2009). The *Populus* homeobox gene *ARBORKNOX2* regulates cell differentiation during secondary growth. *Plant J.* 60, 1000–1014. doi: 10.1111/j.1365-313x.2009.04017.x
- Edgar, R. C. (2004). MUSCLE: multiple sequence alignment with high accuracy and high throughput. *Nucleic Acids Res.* 32, 1792–1797. doi: 10.1093/nar/gkh340
- Ehltng, J., Mattheus, N., Aeschliman, D. S., Li, E., Hamberger, B., Cullis, I. F., et al. (2005). Global transcript profiling of primary stems from *Arabidopsis thaliana* identifies candidate genes for missing links in lignin biosynthesis and transcriptional regulators of fiber differentiation. *Plant J.* 42, 618–640. doi: 10.1111/j.1365-313x.2005.02403.x
- Frankowski, K., Wilmowicz, E., Kućko, A., Zienkiewicz, A., Zienkiewicz, K., and Kopcewicz, J. (2015). Molecular cloning of the *BLADE-ON-PETIOLE* gene and expression analyses during nodule development in *Lupinus luteus*. *Plant Physiol.* 179, 35–39. doi: 10.1016/j.jplph.2015.01.019
- Fu, Z. Q., Yan, S., Saleh, A., Wang, W., Ruble, J., Oka, N., et al. (2012). NPR3 and NPR4 are receptors for the immune signal salicylic acid in plants. *Nature* 486, 228–232. doi: 10.1038/nature11162
- Gietz, R. D., and Schiestl, R. H. (2007). High-efficiency yeast transformation using the LiAc/SS carrier DNA/PEG method. *Nat. Protoc.* 2, 31–34. doi: 10.1038/nprot.2007.13
- Goodstein, D. M., Shu, S., Howson, R., Neupane, R., Hayes, R. D., Fazo, J., et al. (2012). Phytozome: a comparative platform for green plant genomics. *Nucleic Acids Res.* 40, D1178–D1186. doi: 10.1093/nar/gkr944
- Groover, A. T., Mansfield, S. D., DiFazio, S. P., Dupper, G., Fontana, J. R., Millar, R., et al. (2006). The *Populus* homeobox gene *ARBORKNOX1* reveals overlapping mechanisms regulating the shoot apical meristem and the vascular cambium. *Plant Mol. Biol.* 61, 917–932. doi: 10.1007/s11103-006-0059-y
- Haughn, G. W., and Somerville, C. (1986). Sulfonyleurea-resistant mutants of *Arabidopsis thaliana*. *Molec. Gen. Genet.* 204, 430–434. doi: 10.1007/bf00331020
- He, L., Lei, Y., Li, X., Peng, Q., Liu, W., Jiao, K., et al. (2020). *Symmetric petals 1* encodes an ALOG domain protein that controls floral organ internal asymmetry in pea (*Pisum sativum* L.). *Int. J. Mol. Sci.* 21, 1–15. doi: 10.3390/ijms211114060
- Hellens, R. P., Anne Edwards, E., Leyland, N. R., Bean, S., and Mullineaux, P. M. (2000). pGreen: a versatile and flexible binary Ti vector for *Agrobacterium*-mediated plant transformation. *Plant Mol. Biol.* 42, 819–832. doi: 10.1023/a:1006496308160
- Hepworth, S. R., and Pautot, V. A. (2015). Beyond the divide: boundaries for patterning and stem cell regulation in plants. *Front. Plant Sci.* 6. doi: 10.3389/fpls.2015.01052
- Hepworth, S. R., Zhang, Y., McKim, S., Li, X., and Haughn, G. W. (2005). *BLADE-ON-PETIOLE*-dependent signaling controls leaf and floral patterning in Arabidopsis. *Plant Cell* 17, 1434–1448. doi: 10.1105/tpc.104.030536
- Izhaki, A., Alvarez, J. P., Cinnamon, Y., Genin, O., Liberman-Aloni, R., and Eyal, Y. (2018). The tomato *BLADE ON PETIOLE* and *TERMINATING FLOWER* regulate leaf axil patterning along the proximal-distal axes. *Front. Plant Sci.* 9. doi: 10.3389/fpls.2018.01126
- Jansson, S., and Douglas, C. J. (2007). *Populus*: a model system for plant biology. *Annu. Rev. Plant Biol.* 58, 435–458. doi: 10.1146/annrev.arplant58.032806.103956
- Jost, M., Taketa, S., Mascher, M., Himmelbach, A., Yuo, T., Shahinnia, F., et al. (2016). A homolog of *BLADE-ON-PETIOLE 1* and 2 (*BOP1/2*) controls internode length and homeotic changes of the barley inflorescence. *Plant Physiol.* 171, 1113–1127. doi: 10.1104/pp.16.00124
- Jun, J. H., Ha, C. M., and Fletcher, J. C. (2010). *BLADE-ON-PETIOLE1* coordinates organ determinacy and axial polarity in Arabidopsis by directly activating *ASYMMETRIC LEAVES2*. *Plant Cell* 22, 62–76. doi: 10.1105/tpc.109.070763
- Khan, M., Ragni, L., Tabb, P., Salasini, B. C., Chatfield, S., Datla, R., et al. (2015). Repression of lateral organ boundary genes by *PENNYWISE* and *POUND-FOOLISH* is essential for meristem maintenance and flowering in Arabidopsis. *Plant Physiol.* 169, 2166–2186. doi: 10.1104/pp.15.00915
- Khan, M., Tabb, P., and Hepworth, S. R. (2012a). *BLADE-ON-PETIOLE1* and 2 regulate Arabidopsis inflorescence architecture in conjunction with homeobox genes *KNAT6* and *ATH1*. *Plant Signal. Behav.* 7, 788–792. doi: 10.4161/psb.20599
- Khan, M., Xu, H., and Hepworth, S. R. (2014). *BLADE-ON-PETIOLE* genes: setting boundaries in development and defense. *Plant Sci.* 215–216, 157–171. doi: 10.1016/j.plantsci.2013.10.019
- Khan, M., Xu, M., Murmu, J., Tabb, P., Liu, Y., Storey, K., et al. (2012b). Antagonistic interaction of *BLADE-ON-PETIOLE1* and 2 with *BREVIPEDICELLUS* and *PENNYWISE* regulates Arabidopsis inflorescence architecture. *Plant Physiol.* 158, 946–960. doi: 10.1104/pp.111.188573
- Koncz, C., and Schell, J. (1986). The promoter of TL-DNA gene 5 controls the tissue-specific expression of chimaeric genes carried by a novel type of *Agrobacterium* binary vector. *Molec. Gen. Genet.* 204, 383–396. doi: 10.1007/bf00331014
- Liebsch, D., Sunaryo, W., Holmlund, M., Norberg, M., Zhang, J., Hall, H. C., et al. (2014). Class I KNOX transcription factors promote differentiation of cambial derivatives into xylem fibers in the Arabidopsis hypocotyls. *Development* 141, 4311–4319. doi: 10.1242/dev.111369
- Liu, L., Ramsay, T., Zinkgraf, M., Sundell, D., Street, N. R., Filkov, V., et al. (2015). A resource for characterizing genome-wide binding and putative target genes of transcription factors expressed during secondary growth and wood formation in *Populus*. *Plant J.* 82, 887–898. doi: 10.1111/tpj.12850
- Liu, S., Magne, K., Daniel, S., Sibout, R., and Ratet, P. (2022). *Brachypodium distachyon* *UNICULME4* and *LAXATUM-A* are redundantly required for development. *Plant Physiol.* 188, 363–381. doi: 10.1093/plphys/kiab456
- Lu, Q., Tang, X., Tian, G., Wang, F., Liu, K., Nguyen, V., et al. (2009). Arabidopsis homolog of the yeast TREX-2 mRNA export complex: components and anchoring nucleoporin. *Plant J.* 61, 259–270. doi: 10.1111/j.1365-313x.2009.04048.x
- Magne, K., Couzigou, J. M., Schiessl, K., Liu, S., George, J., Zhukov, V., et al. (2018). *MtNODULE ROOT1* and *MtNODULE ROOT2* are essential for indeterminate nodule identity. *Plant Physiol.* 178, 295–316. doi: 10.1104/pp.18.00610
- Magne, K., Liu, S., Massot, S., Dalmais, M., Morin, H., Sibout, R., et al. (2020). Roles of *BdUNICULME4* and *BdLAXATUM-A* in the non-domesticated grass *Brachypodium distachyon*. *Plant J.* 103, 645–659. doi: 10.1111/tpj.14758
- McKim, S. M., Stenvik, G. E., Butenko, M. A., Kristiansen, W., Cho, S. K., Hepworth, S. R., et al. (2008). The *BLADE-ON-PETIOLE* genes are essential for abscission zone formation in Arabidopsis. *Development* 135, 1537–1546. doi: 10.1242/dev.012807
- Murmu, J., Bush, M. J., DeLong, C., Li, S., Xu, M., Khan, M., et al. (2010). Arabidopsis basic leucine-zipper transcription factors TGA9 and TGA10 interact with floral glutaredoxins ROXY1 and ROXY2 and are redundantly required for anther development. *Plant Physiol.* 154, 1492–1504. doi: 10.1104/pp.110.159111
- Nakano, Y., Yamaguchi, M., Endo, H., Rejab, N. A., and Ohtani, M. (2015). NAC-MYB-based transcriptional regulation of secondary cell wall biosynthesis in land plants. *Front. Plant Sci.* 6, 288. doi: 10.3389/fpls.2015.00288
- Nieminen, K., Blomster, T., Helariutta, Y., and Mähönen, A. P. (2015). Vascular cambium development. *Arabidopsis Book* 13, e0177. doi: 10.1199/tab.0177
- Norberg, M., Holmlund, M., and Nilsson, O. (2005). The *BLADE ON PETIOLE* genes act redundantly to control the growth and development of lateral organs. *Development* 132, 2203–2213. doi: 10.1242/dev.01815
- Pfaffl, M. W. (2001). A new mathematical model for relative quantification in real-time RT-PCR. *Nucleic Acids Res.* 29, e45–e45. doi: 10.1093/nar/29.9.e45
- Rogers, L. A., and Campbell, M. M. (2004). The genetic control of lignin deposition during plant growth and development. *New Phytol.* 164, 17–30. doi: 10.1111/j.1469-8137.2004.01143.x
- Sanchez, P., Nehlin, L., and Greb, T. (2012). From thin to thick: major transitions during stem development. *Trends Plant Sci.* 17, 113–121. doi: 10.1016/j.tplants.2011.11.004
- Sannigrahi, P., Ragauskas, A. J., and Tuskan, G. A. (2010). Poplar as a feedstock for biofuels: A review of compositional characteristics. *Biofuel. Bioprod. Biorefin.* 4, 209–226. doi: 10.1002/bbb.206
- Sehr, E. M., Agusti, J., Lehner, R., Farmer, E. E., Schwarz, M., and Greb, T. (2010). Analysis of secondary growth in the Arabidopsis shoot reveals a positive role of jasmonate signalling in cambium formation. *Plant J.* 63, 811–822. doi: 10.1111/j.1365-313x.2010.04283.x
- Shen, D., Holmer, R., Kulikova, O., Mannapperuma, C., Street, N. R., Yan, Z., et al. (2021). The BOP-type co-transcriptional regulator *NODULE ROOT1* promotes stem secondary growth of the tropical Cannabaceae tree *Parasponia andersonii*. *Plant J.* 106, 1366–1386. doi: 10.1111/tpj.15242
- Song, J., Lu, S., Chen, Z. Z., Lourenco, R., and Chiang, V. L. (2006). Genetic transformation of *Populus trichocarpa* genotype Nisqually-1: a functional genomic tool for woody plants. *Plant Cell Physiol.* 47, 1582–1589. doi: 10.1093/pccp/plc018
- Sundell, D., Street, N. R., Kumar, M., Mellerowicz, E. J., Kucukoglu, M., Johnsson, C., et al. (2017). AspWood: High-spatial-resolution transcriptome profiles reveal uncharacterized modularity of wood formation in *Populus tremula*. *Plant Cell* 29, 1585–1604. doi: 10.1105/tpc.17.00153
- Tavakol, E., Okagaki, R., Verderio, G., Vahid, S. J., Hussien, A., Bilgic, H., et al. (2015). The barley *Uniculme 4* gene encodes a *BLADE-ON-PETIOLE*-like protein that controls tillering and leaf patterning. *Plant Physiol.* 168, 164–174. doi: 10.1104/pp.114.252882
- Taylor, G. (2002). *Populus*: Arabidopsis for forestry. Do we need a model tree? *Ann. Bot.* 90, 681–689. doi: 10.1093/aob/mcf255
- Toriba, T., Tokunaga, H., Nagasawa, K., Nie, F., Yoshida, A., and Kyozuka, J. (2020). Suppression of leaf blade development by *BLADE-ON-PETIOLE* orthologs is a

- common strategy for underground rhizome growth. *Curr. Biol.* 30, 509–516. doi: 10.1016/j.cub.2019.11.055
- Toriba, T., Tokunaga, H., Shiga, T., Nie, F., Naramoto, S., Honda, E., et al. (2019). *BLADE-ON-PETIOLE* genes temporally and developmentally regulate the sheath to blade ratio of rice leaves. *Nat. Commun.* 10, 619. doi: 10.1038/s41467-019-08479-5
- Unda, F., Kim, H., Hefer, C., Ralph, J., and Mansfield, S. D. (2017). Altering carbon allocation in hybrid poplar (*Populus alba* × *grandidentata*) impacts cell wall growth and development. *Plant Biotechnol. J.* 15, 865–878. doi: 10.1111/pbi.12682
- Wang, D., Chen, Y., Li, W., Li, Q., Lu, M., Zhou, G., et al. (2021). Vascular cambium: the source of wood formation. *Front. Plant Sci.* 12. doi: 10.3389/fpls.2021.700928
- Wang, S., Li, E., Porth, I., Chen, J. G., Mansfield, S. D., and Douglas, C. J. (2014). Regulation of secondary cell wall biosynthesis by poplar R2R3 MYB transcription factor PtrMYB152 in Arabidopsis. *Sci. Rep.* 4, 5054. doi: 10.1038/srep05054
- Wang, Y., Salasini, B. C., Khan, M., Devi, B., Bush, M., Subramaniam, R., et al. (2019). Clade I TGACG-motif binding basic leucine zipper transcription factors mediate *BLADE-ON-PETIOLE*-dependent regulation of development. *Plant Physiol.* 180, 937–951. doi: 10.1104/pp.18.00805
- Woerlen, N., Allam, G., Popescu, A., Corrigan, L., Pautot, V., and Hepworth, S. R. (2017). Repression of *BLADE-ON-PETIOLE* genes by KNOX homeodomain protein BREVIPEDICELLUS is essential for differentiation of secondary xylem in Arabidopsis root. *Planta* 245, 1079–1090. doi: 10.1007/s00425-017-2663-2
- Wu, X. M., Yu, Y., Han, L. B., Li, C. L., Wang, H. Y., Zhong, N. Q., et al. (2012). The tobacco *BLADE-ON-PETIOLE2* gene mediates differentiation of the corolla abscission zone by controlling longitudinal cell expansion. *Plant Physiol.* 159, 835–850. doi: 10.1104/pp.112.193482
- Xu, C., Park, S. J., Van Eck, J., and Lippman, Z. B. (2016). Control of inflorescence architecture in tomato by BTB/POZ transcriptional regulators. *Genes Dev.* 30, 2048–2061. doi: 10.1101/gad.288415.116
- Žádníková, P., and Simon, R. (2014). How boundaries control plant development. *Curr. Opin. Plant Biol.* 17, 116–125. doi: 10.1016/j.pbi.2013.11.013
- Zhang, B., Holmlund, M., Lorrain, S., Norberg, M., Bakó, L. S., Fankhauser, C., et al. (2017). *BLADE-ON-PETIOLE* proteins act in an E3 ubiquitin ligase complex to regulate PHYTOCHROME INTERACTING FACTOR 4 abundance. *elife* 6, e26759. doi: 10.7554/elife.26759
- Zhang, Z., Wang, P., Luo, X., Yang, C., Tang, Y., Wang, Z., et al. (2019). Cotton plant defence against a fungal pathogen is enhanced by expanding *BLADE-ON-PETIOLE1* expression beyond lateral-organ boundaries. *Commun. Biol.* 2, 238. doi: 10.1038/s42003-019-0468-5
- Zhao, Y., Song, X., Zhou, H., Wei, K., Jiang, C., Wang, J., et al. (2020). *KNAT2/6b*, a class I KNOX gene, impedes xylem differentiation by regulating NAC domain transcription factors in poplar. *New Phytol.* 225, 1531–1544. doi: 10.1111/nph.16036